

Preparation, mechanical properties, and thermal degradation of flame retarded epoxy resins with an organophosphorus oligomer

Xin Wang · Yuan Hu · Lei Song · Weiyi Xing ·
Hongdian Lu

Received: 28 November 2010 / Revised: 5 March 2011 / Accepted: 13 March 2011 /

Published online: 31 March 2011

© Springer-Verlag 2011

Abstract An organophosphorus oligomer, poly(DOPO-substituted hydroxyphenyl methanol pentaerythritol diphosphonate) (PFR), was synthesized from the dehydrohalogenation polycondensation of 9,10-dihydro-9-oxa-10-phosphaphenanthrene-10-oxide substituted hydroxyphenyl methanol (DOPO-HBA) with 3,9-bis(chloro)-2,4,8,10-tetraoxa-3,9-diphosphaspiro [5.5]undecane-3,9-dioxide (SPDPC). The structure of PFR was confirmed by FTIR, ¹H NMR, and ³¹P NMR. Advanced flame retardant epoxy resins (FREP) were obtained by incorporating PFR into EP, cured by 4,4'-diaminodiphenylmethane (DDM). Effects of PFR on thermal, dynamic mechanical properties, and flame retardant properties of the epoxy resins were investigated. The dynamic mechanical analysis (DMA) results showed that EP/PFR exhibited higher glass transition temperature than that of neat EP. Moreover, incorporation of PFR significantly enhanced the char yield at higher temperatures. The addition of PFR into epoxy resins significantly improved their flame retardancy, due to the reduction of peak heat release rate, total heat release as well as the mass loss rate.

Keywords Epoxy resin · Flame retardancy · Thermal degradation · Organophosphorus oligomer · Dynamic mechanical properties

X. Wang · Y. Hu (✉) · L. Song · W. Xing · H. Lu
State Key Laboratory of Fire Science, University of Science and Technology of China,
Hefei, Anhui 230026, People's Republic of China
e-mail: yuanhu@ustc.edu.cn

X. Wang · Y. Hu
Suzhou Key Laboratory of Urban Public Safety, Suzhou Institute for Advanced Study,
University of Science and Technology of China, Suzhou, Jiangsu 215123,
People's Republic of China

H. Lu
Department of Chemical and Materials Engineering, Key Laboratory of Powder and Energy
Materials, Hefei University, Hefei, Anhui 230022, People's Republic of China

Introduction

Owing to their outstanding mechanical stiffness and toughness, good solvent and chemical resistance, and superior adhesion, epoxy resins (EP) are widely used as coatings, adhesives, laminates, semiconductor encapsulation, and matrices for advanced fiber-reinforced composites [1–5]. However, flammability is one of main disadvantages of epoxy resins, which restricts their applications in electronics. Consequently, extensive research has been developed to improve the flame retardant performance of epoxy resins. Traditionally, epoxy resins can be rendered flame retardancy by the incorporation of halogen-containing flame retardants [6–8]. Nevertheless, the utilization of these halogenated flame retardants can generate toxic, corrosive gases, and endocrine-disrupting chemicals during combustion, which is harmful to the environments and human health [9–11]. Therefore, there is an inevitable trend toward using halogen-free flame retardants in epoxy resins.

Among the halogen-free flame retardants, a wide variety of flame retardant epoxy resins with 9,10-dihydro-9-oxa-10-phosphaphenanthrene 10-oxide (DOPO) and its derivatives have attracted extensive attention in recent years [12–15]. DOPO-containing compounds could react with various epoxy monomers and also be found to produce less toxic gas and smoke than halogen-containing compounds. However, the DOPO-containing compounds reported are mostly small molecular flame retardants, which exists many drawbacks, such as leaching and low phosphorus content. Therefore, the polymeric flame retardants, possessing high phosphorus content and rich aromatic structure, are highly noting.

With the aim of improving the flame retardancy of epoxy resins, we synthesized a novel organophosphorus oligomer which contained phosphorus element in both main chain and pendant group, and incorporated it into the epoxy resin systems. This article explored the influence of the organophosphorus oligomer on the flame retardancy of epoxy resins. Their thermal and dynamic mechanical thermal properties were also evaluated.

Experimental

Materials

9,10-Dihydro-9-oxa-10-phosphaphenanthrene 10-oxide (DOPO) was supplied by Shandong Mingshan fine chemical industry company. Epoxy resin (DGEBA, commercial name: E-44) was supplied by Hefei Jiangfeng chemical industry company. Phosphorus oxychloride was reagent grade and provided by Tianjin Guangfu fine chemical research institute (Tianjin, China). Pentaerythritol, 4,4'-diamino-diphenyl methane (DDM), acetonitrile, toluene, 4-hydroxybenzaldehyde (HBA), tetrahydrofuran (THF), trichloromethane, and diethyl ether were all reagent grade and purchased from Sinopharm chemical reagent Co. Ltds (Shanghai, China). Tetrahydrofuran, toluene, and acetonitrile were distilled at reduced pressure before use. DOPO was recrystallized from tetrahydrofuran before use.

Measurement

Fourier transform infrared (FTIR) spectra were recorded on a Nicolet 6700 FTIR spectrophotometer with KBr pellets. Spectra in the optical range of 400–4000 cm⁻¹ were obtained by averaging 16 scans at a resolution of 4 cm⁻¹.

All NMR spectra were performed on a Bruker AV400 NMR spectrometer (400 MHz) operating in the Fourier transform mode using DMSO-*d*₆ as solvent.

Limiting oxygen index (LOI) was measured according to ASTM D2863. The apparatus used was an HC-2 oxygen index meter (Jiangning Analysis Instrument Co., China). The specimens used for the test were of dimensions 100 mm × 6.5 mm × 3 mm. The vertical test was carried out on a CFZ-2 type instrument (Jiangning Analysis Instrument Co., China) according to the UL-94 test standard. The specimens used were of dimensions 130 mm × 13 mm × 3 mm.

Thermogravimetric analysis (TGA) of samples were carried out with Q5000 thermal analyzer (TA Co., USA) under both air and nitrogen atmosphere from 50 °C to 700 °C at a heating rate of 20 °C/min.

Pyrolysis combustion flow calorimetry experiments were carried out on a Govmark MCC-2 microscale combustion calorimeter (MCC). Samples weighing 4 ± 1 mg were heated to 650 °C at a heating rate of 1 °C/s in a stream of nitrogen flowing at 80 mL/min. The combustor temperature was set at 900 °C and oxygen/nitrogen flow rate was set at 20/80 mL/mL. The reported data were averages of three tests and the experimental error was ±5%.

Dynamic mechanical analysis (DMA) was performed with the PerkinElmer Pyris Diamond DMA from 20 to 250 °C at a heating rate of 10 °C/min, at a frequency of 1 Hz in the tensile configuration.

Synthesis of DOPO–HBA

In a 500 mL round-bottom flask, DOPO (21.6 g, 0.1 mol), HBA (13.4 g, 0.11 mol), and dried toluene (200 mL) were introduced and stirred under a nitrogen atmosphere. The mixture was refluxed for about 5 h. The reaction solution then became thick due to the precipitation of the resultant DOPO–HBA. After being cooled to room temperature, the precipitate was filtered and washed with toluene. The obtained solid was then recrystallized from toluene/methanol (2/1 in volume) to give a pure product with a 90% yield.

Fourier transform infrared (FTIR) (KBr, cm⁻¹): 3225 (C–OH); 1590 (P–Ph); 1180 (P=O); 935 (P–O–Ph). ¹H NMR (400 MHz, DMSO-*d*₆): δ 4.97–5.18 (t, *J* = 5.7, 1H), 6.08–6.25 (dd, *J* = 17.8, 5.7, 1H), 6.64–6.73 (dd, *J* = 9.2, 6.3, 2H), 7.05–7.31 (m, 4H), 7.36–7.60 (m, 2H), 7.72–7.80 (m, 1H), 7.85–7.92 (ddd, *J* = 12.2, 7.6, 1.1, 1H), 8.08–8.22 (m, 2H) and 9.40 (m, *J* = 9.8, 1H). ³¹P NMR (400 MHz, DMSO-*d*₆, ppm): 31.1 ppm.

Synthesis of SPDPC

A 500 mL three-necked and round-bottom glass flask equipped with a temperature controller, magnetic stirrer, and a reflux condenser was charged with phosphorus

oxychloride (200 mL) and pentaerythritol (49.5 g). The temperature of the reaction mixture was raised to 75 °C and maintained for 6 h under a nitrogen gas atmosphere. Afterwards, the reaction mixture was heated slowly to 105 °C and maintained for 12 h. After cooling to room temperature, the precipitate was filtered and washed with trichloromethane and diethyl ether. The white powder was collected by filtration, and dried under reduced pressure. The yield of SPDPC was about 85%.

Fourier transform infrared (FTIR) (KBr, cm^{-1}): 1303 (P=O), 1028 (P—O—C), 580 (P—Cl). ^1H NMR (400 MHz, DMSO- d_6): δ 4.22–4.29 (d, $J = 12.3$, 8H). ^{31}P NMR (400 MHz, DMSO- d_6 , ppm): –11.1.

Synthesis of PFR

In a 500 mL three-necked and round-bottom glass flask equipped with a temperature controller, magnetic stirrer, and a reflux condenser, SPDPC (14.9 g), DOPO-HBA (18.6 g), and acetonitrile (250 mL) were mixed at 70 °C for 1 h. Thereafter, the mixture was gradually heated and refluxed until no HCl gas was emitted. The solvent was removed by rotary evaporator under reduced pressure. The raw product obtained was washed by acetonitrile three times. The product was then dried in vacuum drying oven at 60 °C overnight. The yield of PFR was about 71%.

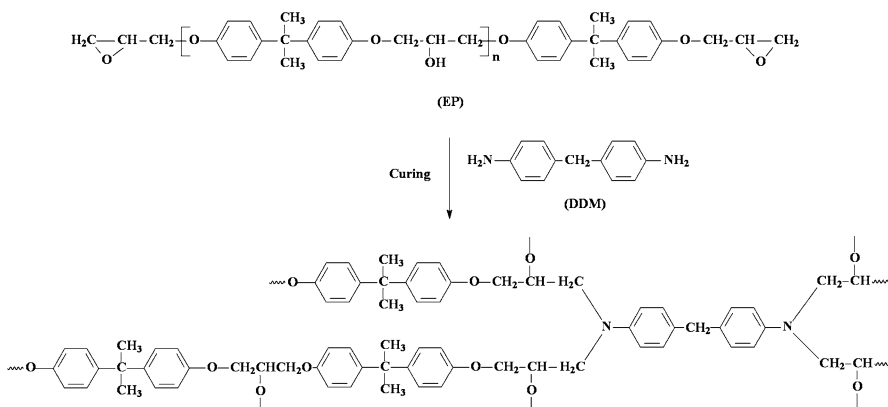
Fourier transform infrared (FTIR) (KBr, cm^{-1}): 3225 (C—OH); 1590 (P—Ph); 1180 (P=O); 935 (P—O—Ph). ^1H NMR (400 MHz, DMSO- d_6): δ 4.13–4.26 (t, $J = 11.2$, 8H), 4.97–5.18 (d, $J = 8.0$, 1H), 6.64–6.73 (dd, $J = 15.4$, 8.5, 2H), 7.05–7.31 (m, 4H), 7.36–7.60 (m, 2H), 7.72–7.80 (m, 1H), 7.85–7.92 (m, 1H) and 8.08–8.22 (m, 2H). ^{31}P NMR (400 MHz, DMSO- d_6 , ppm): 31.0, –7.3, –20.7.

Curing procedure of phosphorus-containing epoxy resins

The phosphorus-containing epoxy resins were formed by blending EP with PFR for 30 min under the vigorous mechanical stirring. Thereafter the above mixture was blended homogeneously with DDM in an epoxide/amino equivalent ratio of 1/1. The compositions of the phosphorus-containing epoxy resins are listed in Table 1. The mixtures were cured at 100 °C for 2 h and post cured at 150 °C for 2 h, and the curing reaction mechanism is shown in Scheme 1. After curing, all samples were cooled to room temperature.

Table 1 Sample formulations and flame retardancy of epoxy resin systems

Sample code	PFR content (wt%)	Flame retardancy	
		LOI	UL-94
EP	0	20.5	Not classified
EP/PFR-1	5	28.5	V-1
EP/PFR-2	10	31.5	V-1
EP/PFR-3	15	33.0	V-0

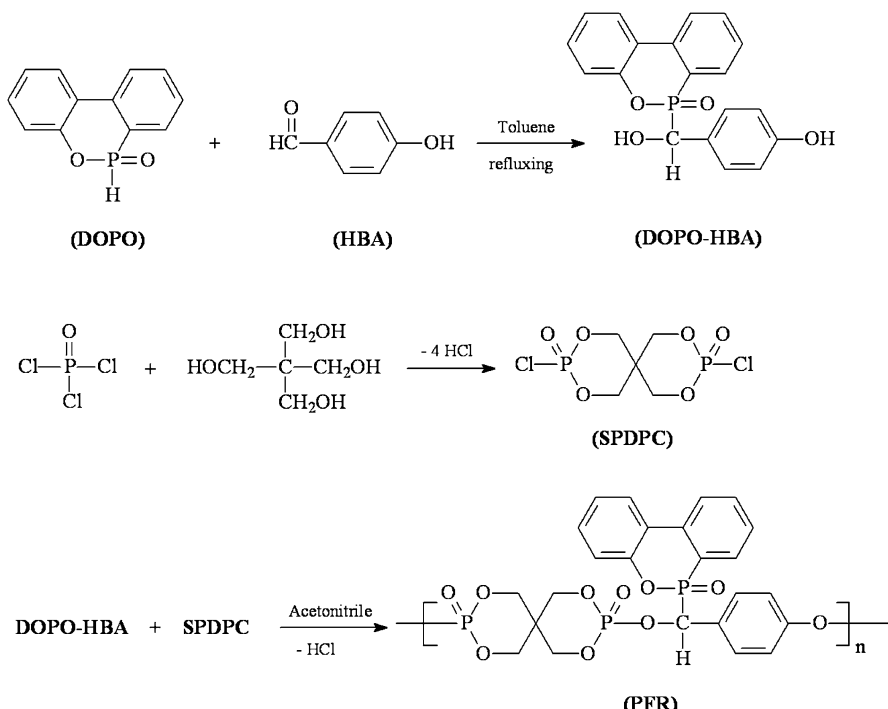
**Scheme 1** Curing reaction between EP and DDM

Results and discussion

Structural characterization of DOPO–HBA and PFR

It is well known that the electrophilic $-P(O)-H$ group in DOPO is reactive toward the nucleophilic $C=O$ in aldehydes and ketones via an electrophilic addition reaction. Therefore, an addition reaction between DOPO and HBA was performed, resulting in the product DOPO–HBA. With the further dehydrohalogenation polycondensation of DOPO–HBA with SPDPC, a DOPO-substituted organophosphorus oligomer (PFR) was obtained (Scheme 2). Figure 1 shows the FTIR spectra for SPDPC, DOPO–HBA, and PFR. As the addition reaction between DOPO and HBA proceeded, the distinctive absorption at 2385 cm^{-1} for P–H stretching in DOPO [9] disappeared, while a broad absorption at around 3232 cm^{-1} for aliphatic OH appeared in DOPO–HBA. Moreover, the specific absorption peak at 580 cm^{-1} (P–Cl) disappeared and some characteristic absorption bands at $1514\text{ (P–Ph), } 1180\text{ (P=O), and } 935\text{ cm}^{-1}$ (P–O–Ph) [9, 16] were observed in the FTIR spectrum of PFR, indicating that the reaction between hydroxyl group and phosphoryl chloride group.

The performance of the addition reaction between HBA and DOPO is further demonstrated by 1H NMR (Fig. 2) with the observation of the absorption peaks at $\delta = 4.97\text{--}5.18\text{ ppm}$ [$P-C-H$] and $\delta = 6.08\text{--}6.25\text{ ppm}$ [$P-C-OH$]. After the occurrence of the dehydrohalogenation reaction between DOPO–HBA and SPDPC, the 1H NMR absorption peaks at $6.08\text{--}6.25\text{ ppm}$ [$P-C-OH$] and 9.40 ppm [$Ph-OH$] disappeared, meanwhile, the absorption peak of $-CH_2-$ in SPDPC shifted from 4.20 ppm to 4.25 ppm . Moreover, DOPO–HBA exhibited only a single peak in ^{31}P NMR spectra (Fig. 3) at $\delta = 31.1\text{ ppm}$, while there were three peaks at $\delta = 31.0$, -7.3 , -20.7 ppm in the ^{31}P NMR spectrum of PFR. These provided another support for the occurrence of a dehydrohalogenation reaction between DOPO–HBA



Scheme 2 Synthetic route of DOPO–HBA, SPDPC, and PFR

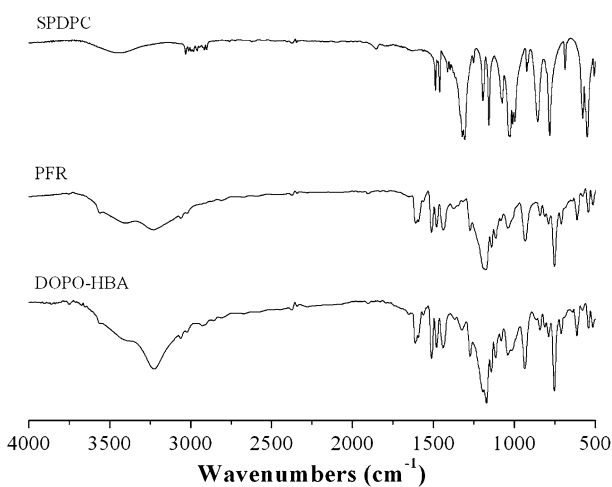


Fig. 1 FTIR spectra of DOPO–HBA, SPDPC, and PFR

and SPDPC. These three peaks also suggested that PFR was DOPO–HBA-terminated. The existence of P–C–OH absorption peak at 3230 cm^{-1} in FTIR spectrum of PFR provided additional evidence.

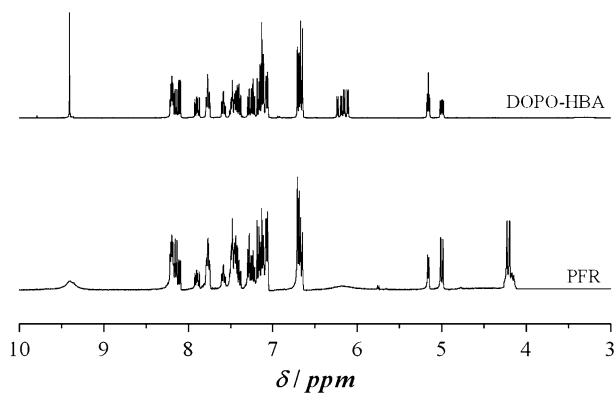


Fig. 2 ^1H NMR spectra of DOPO–HBA and PFR

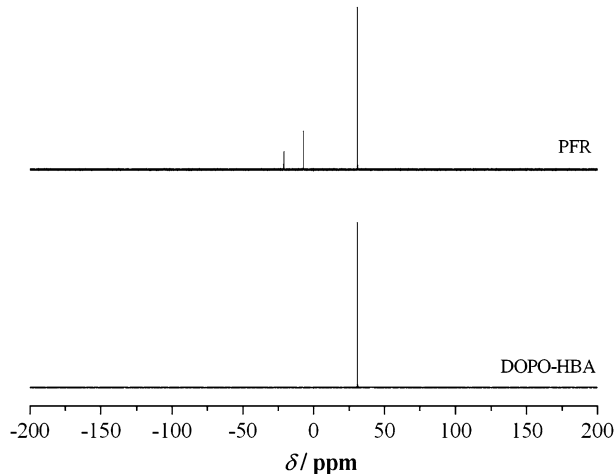


Fig. 3 ^{31}P NMR spectra of DOPO–HBA and PFR

Flame retardancy

To evaluate flame retardancy of EP/PFR systems, Table 1 gives LOI values and vertical burning test (UL-94) results. As can be observed, pure EP was highly combustible, and its LOI value was 20.5%. All EP/PFR composites had higher LOI values than pure EP and the LOI value increased obviously with PFR content. Sample with 15 wt% PFR content produced a UL-94 V-0 material. However, phosphorous-free epoxy resin showed no rating in the burning tests. These results indicated that PFR imparted excellent flame retardant effect to epoxy resins.

Dynamic mechanical properties

Dynamic mechanical analysis (DMA) gives the information about the viscoelastic properties of polymers. The loss factor ($\tan\delta$) versus temperature for the EP and

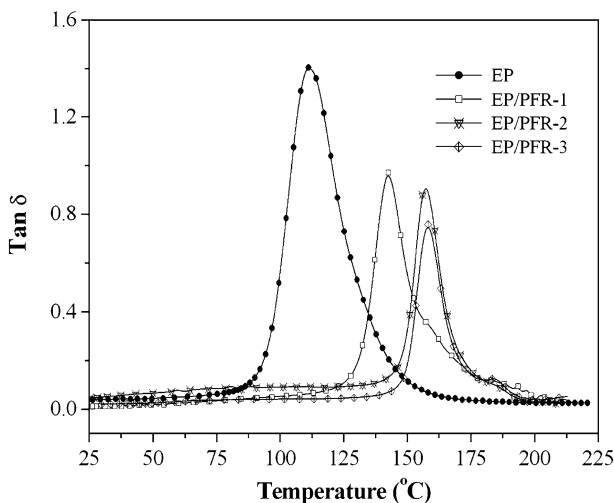


Fig. 4 DMA $\tan\delta$ curves of EP and EP/PFR composites

EP/PFR composites are plotted in Fig. 4. The glass transition temperature (T_g) is obtained as the peak of $\tan\delta$ curve. As can be seen, T_g values increased with the PFR content. Moreover, the height of the $\tan\delta$ peak, which is associated with the crosslinking density [17], decreased as the PFR content increased. Because $\tan\delta$ is the ratio of viscous components to elastic components, it can be assumed that the increased height is associated with higher segmental mobility and more relaxing species. Therefore, it can be concluded that the networks for the PFR-rich samples were tighter.

The storage modulus is closely related to the load bearing capacity of the materials. As shown in Fig. 5, the initial storage modulus had an obvious decrease after incorporating PFR into the EP matrix. The poor interfacial adhesion between the EP matrix and the PFR tended to decrease the crosslinking density of the cured EP/PFR/DDM systems, which may be responsible for the decrease of initial storage modulus. However, for these systems, it should be noted that crosslink density was not the only factor that affected the physical properties of the networks. As far as the chemical structure was concerned, the bulky and rigid structure of PFR displayed a reinforced effect to EP. Consequently, the higher load of PFR gave a positive impact on the storage modulus of EP/PFR composites.

Thermal stability

In order to examine the effect of PFR on the thermal stability of epoxy resins, thermogravimetric analysis (TGA) was measured and analyzed. Figure 6a and b gives TG and DTG curves of epoxy resins with various contents of PFR under air atmosphere, respectively. The temperature at which the weight loss is about 5% is determined as the initial decomposition temperature. The temperature of 5% weight

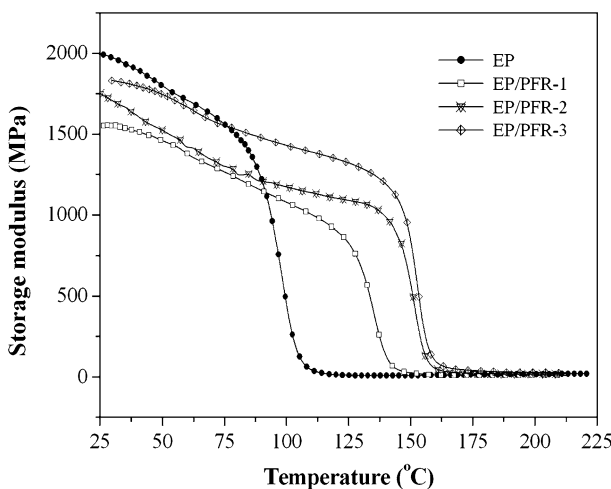


Fig. 5 DMA storage modulus curves of EP and EP/PFR composites

loss ($T_{5\%}$), the temperature of maximum rate of weight loss (T_{\max}), and the percentage of char yield at 700 °C are summarized in Table 2.

As can be observed in Fig. 6, the pure EP started to decompose at 369 °C and the thermal oxidative degradation process mainly had two stages. The first stage was in the temperature range of 350–450 °C corresponding to a strong DTG peak at 380 °C (T_{\max}) and the weight loss was about 59%. The second stage was in the temperature ranges of 500–650 °C corresponding to T_{\max} of 561 °C. As for EP/PFR composites, the thermal oxidative degradation process of all the composites had the similar two stages as the pure EP. However, the temperature of 5% weight loss ($T_{5\%}$) decreased when PFR content increased, which was probably due to the decomposition of P–C bonds which had lower thermal stability than C–C bonds [18]. The major weight loss occurred from about 300 to 450 °C and then weight continued to decrease at a reduced rate from around 450 to 500 °C. This region of intermediate thermal stability reflected the thermal stability of the char layer formed during oxidative degradation. The increased rate of mass loss beyond 500 °C illustrated the continued degradation of the char layer.

Figure 7a and b shows TG and DTG curves of epoxy resins with various contents of PFR under nitrogen atmosphere, respectively. In nitrogen, the thermal degradation process of all the samples was different from that under air because of the presence of inert atmosphere. The thermal degradation process of all the EP/PFR composites had only one stage as the pure EP. When the PFR content increased, $T_{5\%}$ decreased, showing a similar trend to the one mentioned above. From the DTG curves, it can be seen that both in air (Fig. 6b) and inert (Fig. 7b) atmosphere, the weight loss rate of the phosphorus-containing resin was significantly lower than that of the phosphorus-free resin. This behavior was in accordance with the mechanism of improved flame retardance via phosphorus modification: the PFR could catalyze the polymer matrix to form an insulating

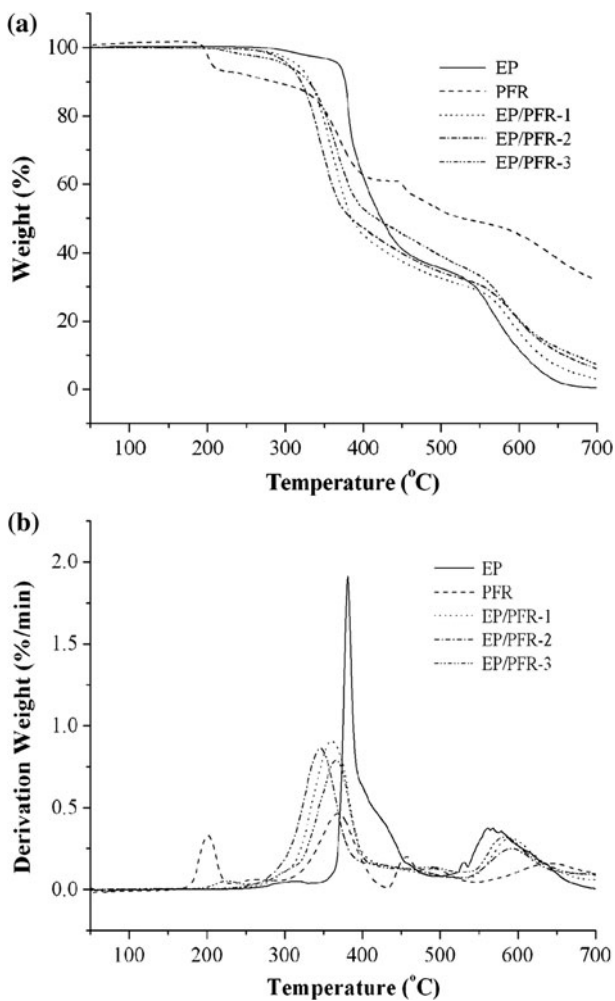


Fig. 6 TGA curves of EP and EP/PFR composites under air atmosphere

Table 2 TGA data of EP and EP/PFR systems

Sample	Nitrogen			Air		
	T _{5%} (°C)	T _{max} (°C)	Char ^a (%)	T _{5%} (°C)	T _{max} (°C)	Char ^a (%)
EP	372	384	13.3	369	380, 561	0.4
PFR	205	201, 389	31.0	206	201, 369, 456	32.0
EP/PFR-1	311	375	19.9	316	361, 592	3.0
EP/PFR-2	321	361	21.5	305	345, 593	6.5
EP/PFR-3	309	350	23.6	301	365, 583	7.4

^a Char yield at 700 °C

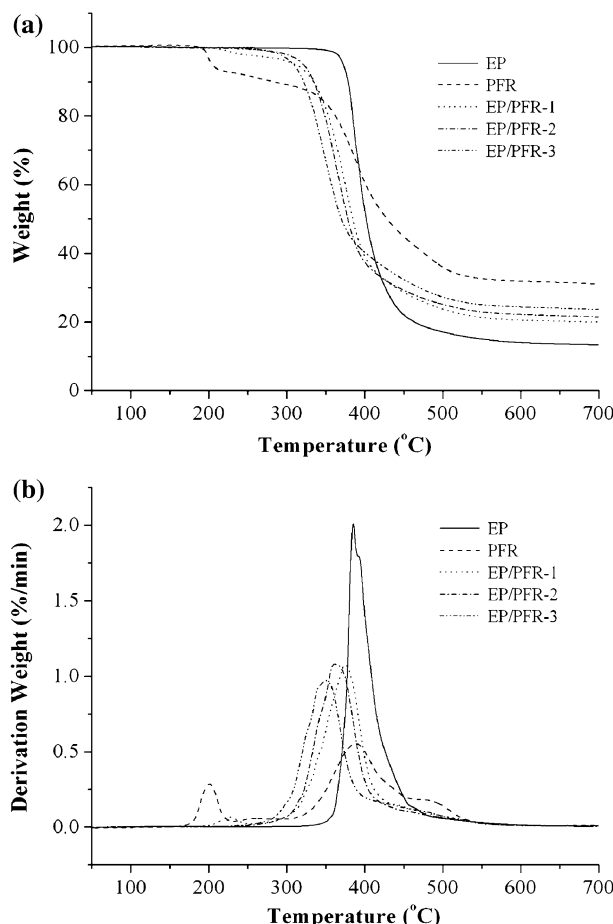


Fig. 7 TGA curves of EP and EP/PFR composites under nitrogen atmosphere

Table 3 MCC data of EP and EP/PFR systems

Sample	HRC (J/gK)	PHRR (W/g)	THR (kJ/g)	T_p (°C)
EP	478	478	20.7	401
EP/PFR-1	287	282	21.1	376
EP/PFR-2	236	235	19.5	357
EP/PFR-3	219	217	16.3	373

protective layer and this char layer reduced the weight loss rate, increased the thermal stability at higher temperatures, and improved the fire retardancy. Char yield under nitrogen is correlated to the polymer's flame retardancy [19] and the char yield increased significantly with the PFR content.

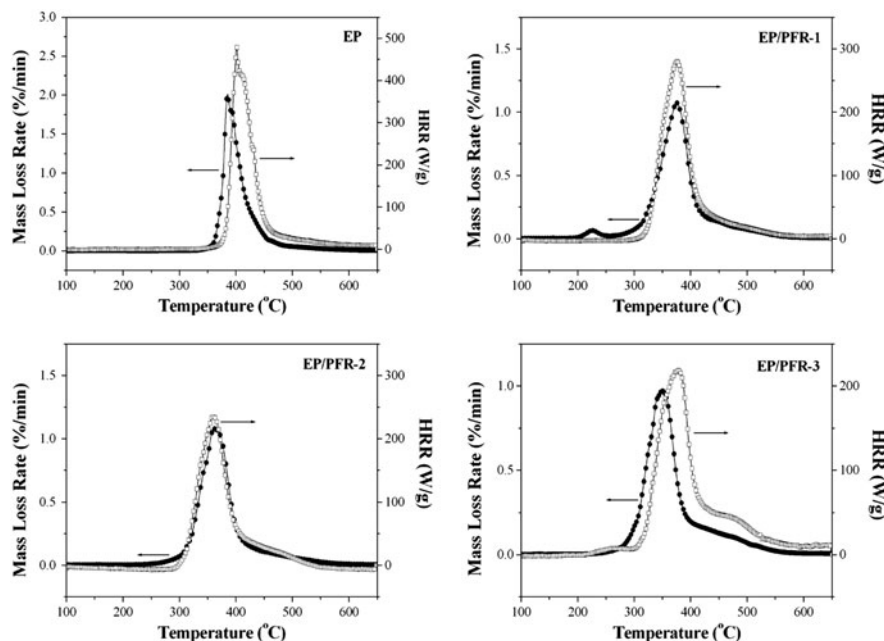


Fig. 8 Comparison of MCC and DTG curves for EP and EP/PFR composites

Microscale combustion calorimeter (MCC) studies

Microscale combustion calorimeter (MCC) is a new, rapid, lab scale test that uses thermal analysis methods to measure chemical properties related to fire. From just a few milligrams of samples, MCC can quickly and easily obtain the key flammability parameters of the materials, such as peak heat release rate (PHRR), heat release capacity (HRC), total heat release (THR), and temperature at PHRR (T_p) [20, 21].

The HRC values, obtained as sum of the two peak heat release rate (HRR) values, are summarized in Table 3. Neat EP showed the highest HRC of 478 J/gK and the highest PHRR of 478 W/g. The sample EP/PFR-1, which contained 5 wt% PFR, showed HRC value of 287 W/g. Addition of PFR led to further reduction in HRC and PHRR and the sample with 15 wt% PFR content exhibited the lowest HRC value, corresponding to about 54.2% reduction in the HRC of neat EP.

Total heat release (THR), calculated from the total area under the HRR peaks, is another important parameter used to evaluate fire hazard. Neat EP exhibited the highest THR of 20.7 kJ/g. In the case of EP/PFR composites, incorporation of PFR into EP led to the reduction of THR. It can be concluded that the addition of PFR was beneficial for reducing the HRC and THR of EP during combustion.

Figure 8 shows the HRR curves from the MCC compared to the DTG curves under nitrogen for EP and EP/PFR composites. It was interesting to find that HRR curve of each sample had the similar shape as DTG curve. Each sample showed a single degradation step in DTG, and only one HRR–MCC peak was observed in the

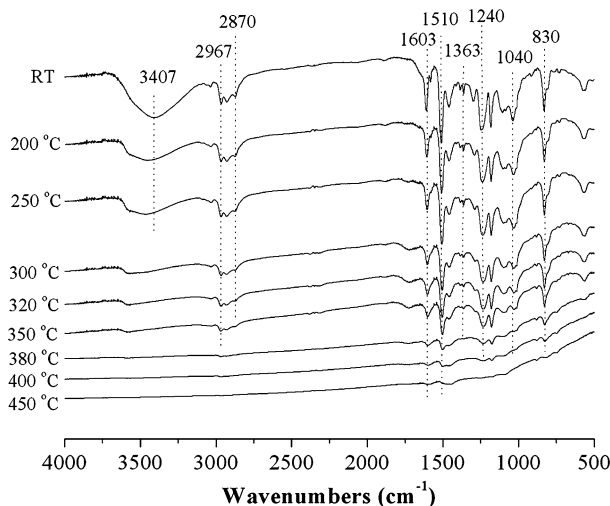


Fig. 9 Real time FTIR spectra of EP at different pyrolysis temperatures

HRR curve. As can be seen that incorporation of PFR into EP could reduce the mass loss rate effectively, as well as the heat release rate during combustion.

Thermal degradation of EP and EP/PFR composites

Real time Fourier transform infrared spectra were employed to explore the details of the thermal oxidative behavior of EP and EP/PFR composite. Figure 9 shows the real time FTIR spectra of EP. Peaks at 3407, 2967, 2870, 1603, 1510, 1363, 1240, 1180, and 1040 cm⁻¹ were the characteristic absorptions of EP. The band at 3403 cm⁻¹ nearly disappeared at the temperature of 250 °C, and this can be explained by the release of water. The relative intensities of the peak at 1363 cm⁻¹ for C-H bond in the C(CH₃)₂ group decreased gradually with temperature increasing from 200 to 320 °C and disappeared completely above 350 °C, indicating that methyl side groups of EP were released. While the temperature rose up to 380 °C, it was found that the absorption peaks at 2967, 2870, 1603, 1510, 1363, 1240, 1180, and 1040 cm⁻¹ nearly disappeared, suggesting that the main decomposition happened at this stage. This is consistent with the TGA results.

Real time FTIR spectra of EP/PFR-3 is presented in Fig. 10. The characteristic peaks of EP/PFR-3 included 2967, 2870, 1603, 1510, 1363, 1240, 1030, and 930 cm⁻¹. It can be found that the relative intensities of CH₃ stretching vibration at 2967, 2870 cm⁻¹ and CH₃ deformation vibration at 1363 cm⁻¹ decreased gradually from 200 to 320 °C and disappeared completely above 350 °C. Meanwhile, the peak at 930 cm⁻¹ assigned to P–O–C bond decreased rapidly above 200 °C and then disappeared completely above 300 °C, indicating that the P–O–C bond in PFR was not stable when heated. It was worth noting that the peaks at 1603, 1510, 830, 750 cm⁻¹ still existed at high temperature region (above 350 °C), implying the formation of aromatic structures. The addition of PFR could promote the formation

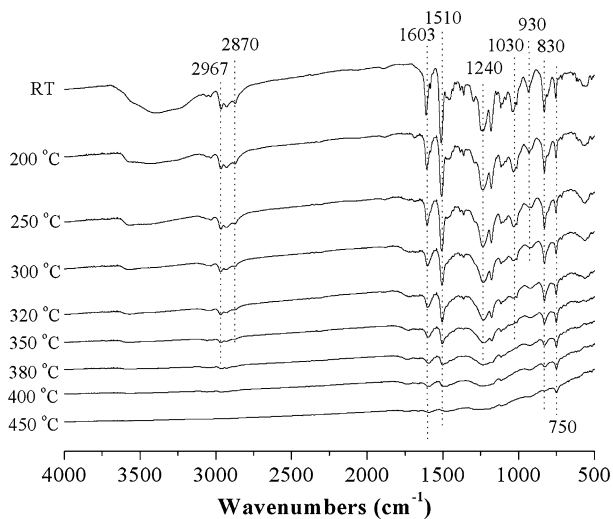


Fig. 10 Real time FTIR spectra of EP/PFR-3 at different pyrolysis temperatures

of char and the residual char can prevent the materials from further degradation during combustion. These results are in good agreement with the data obtained from TGA and MCC.

Conclusions

An organophosphorus oligomer (PFR) was synthesized from the dehydrohalogenation polycondensation of DOPO–HBA with SPDPC. A series of flame retardant epoxy resins with different PFR contents were prepared by crosslinking with DDM. The LOI values increased from 20.5% for the pure EP to 33.0% for phosphorus-containing resins, and UL-94 V-0 materials were obtained with a PFR content of 15 wt%. T_g values of advanced EP/PFR composites increased with the PFR content, but the initial storage modulus was lower than pure EP. TGA results indicated that the char yield and the thermal stability of the char increased with PFR content. The MCC data showed that the incorporation of PFR could significantly reduce the peak heat release rate and total heat release of the epoxy resins during combustion. The comparison between DTG curves and the HRR curves indicated that the EP/PFR composites exhibited decreased mass loss rate and heat release rate when compared to the pure epoxy resins. The thermal degradation behavior showed that DOPO group in PFR first degraded and catalyzed the degradation of the composite to form the protective char layer. This char layer can retard the inner polymer degradation and combustion, thus the fire resistance of epoxy resins was improved.

Acknowledgments The work was financially supported by National Natural Science Foundation of China (No.51036007), the joint fund of NSFC and CAAC (No. 61079015) and the youth innovation fund of USTC.

References

1. Wu CS, Liu YL, Chiu YS (2002) Epoxy resins possessing flame retardant elements from silicon incorporated epoxy compounds cured with phosphorus or nitrogen containing curing agents. *Polymer* 43:4277–4284
2. Wu CS, Liu YL, Hsu KY (2003) Maleimide-epoxy resins: preparation, thermal properties, and flame retardance. *Polymer* 44:565–573
3. Kong J, Tang YS, Zhang XJ, Gu JW (2008) Synergic effect of acrylate liquid rubber and bisphenol A on toughness of epoxy resins. *Polym Bull* 60:229–236
4. Shieh JY, Wang CS (2001) Synthesis of novel flame retardant epoxy hardeners and properties of cured products. *Polymer* 42:7617–7625
5. Jeng RJ, Lo GS, Chen CP, Liu YL, Hsieh GH, Su WC (2003) Enhanced thermal properties and flame retardancy from a thermosetting blend of a phosphorus-containing bismaleimide and epoxy resins. *Polym Adv Technol* 14:147–156
6. Levchik S, Piotrowski A, Weil E, Yao Q (2005) New developments in flame retardancy of epoxy resins. *Polym Degrad Stab* 88:57–62
7. Liu YF, Zhao M, Shen SG, Gao JG (1998) Curing kinetics, thermal property, and stability of tetrabromo-bisphenol-A epoxy resin with 4,4'-diaminodiphenyl ether. *J Appl Polym Sci* 70: 1991–2000
8. Barontini F, Cozzani V, Marsanich K, Raffa V, Petarca L (2004) An experimental investigation of tetrabromobisphenol A decomposition pathways. *J Anal Appl Pyrolysis* 72:41–53
9. Ai H, Xu K, Liu H, Chen MC (2009) Preparation and properties of novel phosphorus-containing binaphthyl epoxy polymer. *Polym Eng Sci* 49:1879–1885
10. Ho TH, Hwang HJ, Shieh JY, Chung MC (2009) Thermal, physical and flame-retardant properties of phosphorus-containing epoxy cured with cyanate ester. *React Funct Polym* 69:176–182
11. Alcon MJ, Ribera G, Galia M, Cadiz V (2005) Advanced flame-retardant epoxy resins from phosphorus-containing diol. *J Polym Sci A* 43:3510–3515
12. Wang CS, Lin CH (2000) Synthesis and properties of phosphorus containing advanced epoxy resins. *J Appl Polym Sci* 75:429–436
13. Ding JP, Tao ZQ, Zuo XB, Fan L, Yang SY (2009) Preparation and properties of halogen-free flame retardant epoxy resins with phosphorus-containing siloxanes. *Polym Bull* 62:829–841
14. Lin CH, Cai SX, Lin CH (2005) Flame-retardant epoxy resins with high glass-transition temperatures. II. Using a novel hexafunctional curing agent: 9,10-dihydro-9-oxa-10-phosphaphenanthrene 10-yl-tris(4-aminophenyl) methane. *J Polym Sci A* 43:5971–5986
15. Artner J, Ciesielski M, Walter O, Doring M, Perez RM, Sandler JKW, Altstadt V, Schartel B (2008) A novel DOPO-based diamine as hardener and flame retardant for epoxy resin systems. *Macromol Mater Eng* 293:503–514
16. Wang CS, Shieh JY (1999) Phosphorus-containing epoxy resin for an electronic application. *J Appl Polym Sci* 73:353–361
17. Huang ZG, Shi WF (2007) UV curing behavior of hyperbranched polyphosphate acrylate/di(hydroxylpropyl methacrylate) piperazine and properties of the cured film. *Prog Org Coat* 59: 312–317
18. Quittmann U, Lecamp L, El Khatib W, Youssef B, Bunel C (2001) Synthesis of a new phosphonated dimethacrylate: photocuring kinetics in homo- and copolymerization, determination of thermal and flame-retardant properties. *Macromol Chem Phys* 202:628–635
19. Espinosa MA, Galia M, Cadiz V (2004) Novel flame-retardant thermosets: phosphine oxide containing diglycidylether as curing agent of phenolic novolac resins. *J Polym Sci A* 42:3516–3526
20. Walters RN, Lyon RE (2003) Molar group contributions to polymer flammability. *J Appl Polym Sci* 87:548–563
21. Shi Y, Kashiwagi T, Walters RN et al (2009) Ethylene vinyl acetate/layered silicate nanocomposites prepared by a surfactant-free method: enhanced flame retardant and mechanical properties. *Polymer* 50:3478–3487